BEM Implementations for an Orthotropic Plate Involving an Elliptical Hole

NECLA KADIOGLU and SENOL ATAOGLU
Department of Civil Engineering
Istanbul Technical University
Division of Mechanics, Faculty of Civil Engineering, Maslak 34469 Istanbul
TURKEY

Abstract: - In this study, an improvement is introduced to solve the linear orthotropic plane problems using boundary element method. This method gives a singular integral equation with complex kernels which will be solved numerically. An artificial boundary is defined to eliminate the singularities and also an algorithm is introduced to calculate multi-valued complex functions which belonged to the kernels of the integral equation. The chosen sample problem is a plate, containing an elliptical hole, stretched by the forces parallel to one of the principal directions of the material. Results are compatible with the solutions given by Lekhnitskii for an infinite plane. Stress distributions have been calculated inside and on the boundary. There is no boundary layer effect.

Key-Words: - elasticity, orthotropic materials, plates having elliptical holes, multi-valued function, boundary element method, singularity

1 Introduction

Analytical solutions of some basic problems of orthotropic elasticity were comprehensively investigated by Lekhnitskii [1-3]. The use of Somigliana' s integral identity is an effective method for the solutions of anisotropic elasticity problems. This method gives an integral equation. In the absence of the body forces this equation involves only surface integrals. Boundary Element Method deals with the numerical solution of this integral equation.

Mantič & París [4] presented a complex formulation of the fundamental displacements and tractions following Lekhnitskii and Stroh theories. Raju et al. [5] presented a method for two-dimensional orthotropic problems.

Some singularity problems arise in the solution of the integral equation mentioned above. Besides, there are some difficulties in the calculation of the unknown stress component on the boundary. This problem is named as boundary layer effect. In this study, whole singularities are eliminated and the unknown stress component are calculated on the boundary. In the previous studies of Kadioglu and Ataoglu [6,7], these two problems had been solved for isotropic and orthotropic materials, respectively. Here, in addition, a new algorithm is also introduced to calculate multi-valued complex functions. The fundamental solution, given by Mantič & París [4], is partially used in this study. A specific problem is solved to check accuracy of the formulation. The present results are seen to be obviously better than those obtained by others, and, they are compatible with Lekhnitskii' s [1-3]. It is noted that there are some mistakes in Lekhnitskii' s book [2] in the theoretical solution of the elliptical hole problem in an infinite plate.

2 Basic Formulations

The definition of a plane problem of orthotropic elasticity is summarized below.

A region B with interior volume V and boundary S is considered. The material filling V is orthotropic. The ordered pair $\mathcal{S}[\boldsymbol{u}(\boldsymbol{x}), \boldsymbol{T}(\boldsymbol{x})]$ define a problem in region B. $\boldsymbol{u}(\boldsymbol{x})$, $\boldsymbol{T}(\boldsymbol{x})$ denote the displacement vector and the stress tensor, respectively. $\boldsymbol{x}$ is the position vector of an arbitrary point. For an orthotropic material, they satisfy following relations.

$$T_{kj,j} + f_k = 0 \tag{1}$$

$$\varepsilon_{kj} = \frac{1}{2}\left(\frac{\partial u_k}{\partial x_j} + \frac{\partial u_j}{\partial x_k}\right) \ (k, j = 1, 2) \tag{2}$$

$$\begin{aligned}\varepsilon_{11} &= \beta_{11}T_{11} + \beta_{12}T_{22}\\ \varepsilon_{22} &= \beta_{12}T_{11} + \beta_{22}T_{22}\\ \varepsilon_{12} &= \frac{1}{2}\beta_{66}T_{12}\end{aligned} \quad (3)$$

where $\boldsymbol{\varepsilon}$ is the strain tensor, β_{kj} represents the elastic constants of the material. $\boldsymbol{f}$ denotes the body force density. The expression of reciprocal identity which is written between two different problems, $\mathcal{S}(\boldsymbol{u},\boldsymbol{T})$ and $\mathcal{S}^*(\boldsymbol{u}^*,\boldsymbol{T}^*)$, for the same body is

$$\int_S \boldsymbol{t}^* \cdot \boldsymbol{u}\, dS + \int_V \boldsymbol{f}^* \cdot \boldsymbol{u}\, dV$$

$$= \int_S \boldsymbol{t} \cdot \boldsymbol{u}^*\, dS + \int_V \boldsymbol{f} \cdot \boldsymbol{u}^*\, dV \quad (4)$$

$$t_k = T_{kj}n_j \ , \ \ {t_k}^* = {T_{kj}}^* n_j \quad (5)$$

$\boldsymbol{t}$ and $\boldsymbol{t}^*$ are surface traction vectors in two problems respectively, $\boldsymbol{n}$ is the outward normal of the surface S. It will be considered that $\mathcal{S}(\boldsymbol{u},\boldsymbol{T})$ represents a problem to be solved on the region B of volume V bounded by surface S. In plane problems, V is reduced to a simple or multiply connected planar region. From now on, $\mathcal{S}(\boldsymbol{u},\boldsymbol{T})$ is considered as the first boundary value problem [8]. But the solution method can be applied to the second boundary value and mixed boundary value problems as well. The second problem $\mathcal{S}^*(\boldsymbol{u}^*,\boldsymbol{T}^*)$ is named as a fundamental or singular solution and it represents the displacement and stress fields in an unbounded plane medium due to a point load applied at a specific point $\boldsymbol{y}$.

3 Fundamental Solution

A body force in an orthotropic, infinite, planar medium having the same elastic constants with the problem to be solved is defined as

$$\boldsymbol{f}^k = \delta(\boldsymbol{x}-\boldsymbol{y})\boldsymbol{e}_k \quad (6)$$

where $\boldsymbol{x}$ and $\boldsymbol{y}$ represent the position vectors of an arbitrary point and a specific point of the medium respectively. $\boldsymbol{e}_k$ $(k=1,2)$ indicates a base vector in Cartesian coordinates. $\delta(\boldsymbol{x}-\boldsymbol{y})$ is a generalized function, which is known as Dirac delta function satisfying the following property:

$$\begin{aligned}\int_V \boldsymbol{h}(\boldsymbol{x})\delta(\boldsymbol{x}-\boldsymbol{y})dV_x &= \boldsymbol{h}(\boldsymbol{y}) \quad for\ \boldsymbol{y}\in V\\ &= \boldsymbol{0} \qquad for\ \boldsymbol{y}\notin V\end{aligned} \quad (7)$$

The solution of this problem can be represented as $\mathcal{S}^k(\boldsymbol{u}^k,\boldsymbol{T}^k)$. This solution is given by Ref. [4] for different types of orthotropic materials as below.

$${u^k}_l(\boldsymbol{x},\boldsymbol{y}) = Re\left\{(\frac{1}{i\pi})\sum_{\lambda=1}^{2} P_{l\lambda}P_{k\lambda}(lnz_\lambda/\kappa_\lambda^2)\right\} \quad (8)$$

$${t^k}_l(\boldsymbol{x},\boldsymbol{y}) = -\frac{1}{\pi i}$$

$$Re\left\{\sum_{\lambda=1}^{2}\frac{1}{\kappa_\lambda^2}P_{k\lambda}Q_{l\lambda}(1/z_\lambda)(\mu_\lambda n_1 - n_2)\right\} \quad (9)$$

where $i=\sqrt{-1}$. The quantities in these two expressions are defined depending on two complex constants $\mu_\lambda(\lambda=1,2)$, defined in terms of β_{ij} coefficients, as the two of the roots of the following nonlinear equation [2,4].

$$\beta_{11}\mu^4 + (2\beta_{12}+\beta_{66})\mu^2 + \beta_{22} = 0 \quad (10)$$

There are two cases for μ_λ values $(\lambda=1,2)$ for

$$(2\beta_{12}+\beta_{66}) > 2\sqrt{\beta_{11}\beta_{22}}$$

$$\mu_1 = \frac{i}{\sqrt{2\beta_{11}}}$$

$$\sqrt{2\beta_{12}+\beta_{66}+\sqrt{(2\beta_{12}+\beta_{66})^2-4\beta_{11}\beta_{22}}}$$

$$\mu_2 = \frac{i}{\sqrt{2\beta_{11}}}$$

$$\sqrt{2\beta_{12}+\beta_{66}+\sqrt{(2\beta_{12}+\beta_{66})^2-4\beta_{11}\beta_{22}}} \quad (11)$$

for $(2\beta_{12}+\beta_{66}) < 2\sqrt{\beta_{11}\beta_{22}}$

$$\mu_1 = c + id \quad , \quad \mu_2 = -c + id$$

where

$$c = \frac{1}{\sqrt{2\beta_{11}}}\sqrt{\sqrt{\beta_{11}\beta_{22}} - (\beta_{12}+\frac{\beta_{66}}{2})}$$
$$d = \frac{1}{\sqrt{2\beta_{11}}}\sqrt{\sqrt{\beta_{11}\beta_{22}} + (\beta_{12}+\frac{\beta_{66}}{2})} \qquad (12)$$

In terms of μ_λ values, $\boldsymbol{Q}$, $\boldsymbol{P}$ and $\boldsymbol{\kappa}$ constant matrices are defined as follows:

$$\boldsymbol{Q} = \begin{bmatrix} -\mu_1 & -\mu_2 \\ 1 & 1 \end{bmatrix}$$

$$\boldsymbol{P} = \begin{bmatrix} \beta_{11}\mu_1^2 + \beta_{12} & \beta_{11}\mu_2^2 + \beta_{12} \\ \beta_{12}\mu_1 + \dfrac{\beta_{22}}{\mu_1} & \beta_{12}\mu_2 + \dfrac{\beta_{22}}{\mu_2} \end{bmatrix} \qquad (13)$$

$$\boldsymbol{\kappa} = \boldsymbol{P}^T\boldsymbol{Q} + \boldsymbol{Q}^T\boldsymbol{P} = \begin{bmatrix} \kappa_1^2 & 0 \\ 0 & \kappa_2^2 \end{bmatrix}$$

$$= 4i\sqrt{\beta_{11}\beta_{22} - (\beta_{12}+\frac{\beta_{66}}{2})^2}\begin{bmatrix} -\mu_1 & 0 \\ 0 & \mu_2 \end{bmatrix} \qquad (14)$$

There are only two $z_\lambda (\lambda = 1, 2)$ variables in Eqs. (8) and (9) defined as

$$z_\lambda = (x_1 - y_1) + \mu_\lambda (x_2 - y_2) \qquad (15)$$

For a first boundary value problem, $\mathcal{S}(\boldsymbol{u}, \boldsymbol{T})$, in orthotropic plane elasticity the expression of the reciprocal identity, equation (4), which is written between $\mathcal{S}(\boldsymbol{u}, \boldsymbol{T})$ and $\mathcal{S}^* = \mathcal{S}^k(\boldsymbol{u}^k, \boldsymbol{T}^k)$, neglecting body forces, is reduced to the following form:

$$\int_S \boldsymbol{t}(\boldsymbol{x}) \cdot \boldsymbol{u}^k(\boldsymbol{x}, \boldsymbol{y}) dS_x - \int_S \boldsymbol{u}(\boldsymbol{x}) \cdot \boldsymbol{t}^k(\boldsymbol{x}, \boldsymbol{y}) dS_x$$

$$\begin{aligned} &= u_k(\boldsymbol{y}) \quad for \quad \boldsymbol{y} \in V, \boldsymbol{y} \notin S \\ &= 0 \qquad for \quad \boldsymbol{y} \notin V, \boldsymbol{y} \notin S \end{aligned} \qquad (16)$$

Using Eq. (16) and Eq. (2) the components of the strain tensor become

$$\varepsilon_{lj}(\boldsymbol{y}) = \frac{1}{2}\int_S \boldsymbol{t}(\boldsymbol{x}) \cdot (\boldsymbol{u}^{lj}(\boldsymbol{x}, \boldsymbol{y}) + \boldsymbol{u}^{jl}(\boldsymbol{x}, \boldsymbol{y})) dS_x$$

$$- \frac{1}{2}\int_S \boldsymbol{u}(\boldsymbol{x}) \cdot (\boldsymbol{t}^{lj}(\boldsymbol{x}, \boldsymbol{y}) + \boldsymbol{t}^{jl}(\boldsymbol{x}, \boldsymbol{y})) dS_x$$

$$for \ \ \mathbf{y} \in V \ \ or \ \ \mathbf{y} \in S \qquad (17)$$

where

$$\boldsymbol{u}^{kj}{}_l(\boldsymbol{x}, \boldsymbol{y}) = \frac{\partial u^k{}_l(\boldsymbol{x}, \boldsymbol{y})}{\partial y_j} =$$

$$- Re\left\{(\frac{1}{i\pi})\sum_{\lambda=1}^{2} P_{k\lambda}P_{l\lambda}(1/\kappa_\lambda^2)(1/z_\lambda)\frac{\partial z_\lambda}{\partial x_j}\right\} \qquad (18)$$

$$t^{kj}{}_l(\boldsymbol{x}, \boldsymbol{y}) = \frac{\partial t^k{}_l(\boldsymbol{x}, \boldsymbol{y})}{\partial y_j} = Re\left\{(1/i\pi)\right.$$

$$\left.\sum_{\lambda=1}^{2} P_{k\lambda}Q_{l\lambda}(1/\kappa_\lambda^2)(1/z_\lambda^2)\frac{\partial z_\lambda}{\partial x_j}(\mu_\lambda n_1 - n_2)\right\} \qquad (19)$$

For the first fundamental problem [8], the surface traction vector $\boldsymbol{t}(\boldsymbol{x})$ is given on the boundary S of the region V. The expressions (8), (9) and (11) to (15) can be found in Ref. [4]. But the right-side of Eq. (16) has been given as $C_{kl}u_l(\mathbf{y})$ for $\mathbf{y} \in S, \mathbf{y} \notin V$ in their study. This term is named as free term in literature and C_{kl} is kl component of $\mathbf{C}$ matrix. The details have been given in Ref. [4]. But their formulation involving $\mathbf{C}$ matrix has not been used in this study.

For a multiply connected region, the boundary S contains a finite number of disjoint curves and an integral over S is equal to the summation of the integrals over these disjoint curves. It is clear that, for the first fundamental problem, the displacement vector can be calculated from Eq. (16) at any arbitrary point $\boldsymbol{y}$ of the region if the displacement field is known on the boundary. Then using Eqs. (17) and (3), the stress components can be calculated at $\boldsymbol{y}$. In that case, the solution of the problem is reduced to calculate the displacement field $\boldsymbol{u}(\boldsymbol{x})$ on the boundary S by solving integral equation given in Eq. (16). The solution of this integral equation is explained below:

Boundary S is idealized as a collection of line segments. If the number of these line segments is N, the number of the end points, named as

nodal points is also N for a closed boundary. It is assumed that the variation of any displacement component on a line segment is linear. Then the unknowns of the problem are reduced to the values of the displacement components at nodal points. $2N$ integral equations each one of them corresponding to a singular loading at a nodal point in one direction can be written. In these integral equations, integrals over the boundary are transformed to the summation of the integrals over the line segments. In addition, an artificial boundary including all of the line segments but not the nodal point $\boldsymbol{x}(I)$, will be defined for a singular loading on that nodal point (Fig. 1). Around $\boldsymbol{x}(I)$ a small circular arc, S_ε, which leaves the point outside the region is added to complete this artificial boundary.

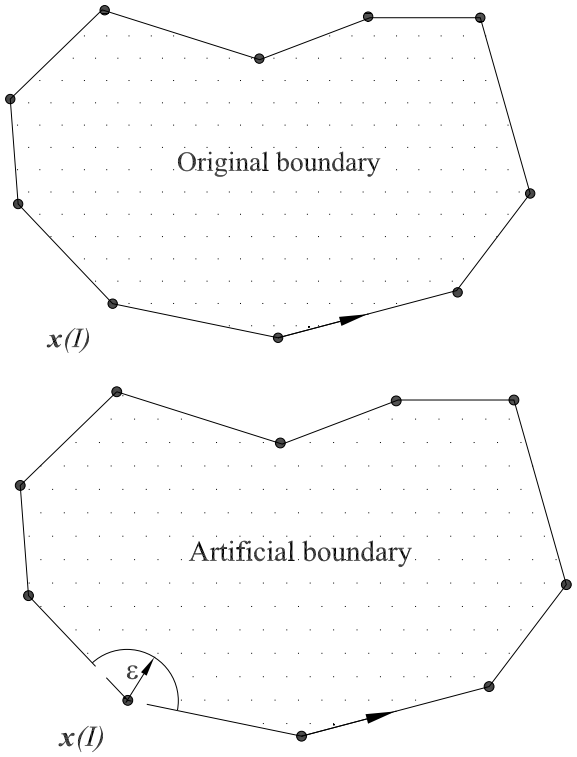

Fig. 1.
Representation of the artificial boundary

It is assumed that the displacement components are constant and the components of surface traction vector are equal to zero on this circular arc S_ε. As a consequence of the definition of the artificial boundary if $\boldsymbol{y}$ is a nodal point $\boldsymbol{x}(I)$, right side of the Eq. (16) becomes zero because $\boldsymbol{y}$ is not a point in the region bounded by this artificial boundary. After necessary calculations the radius ε of the circular arc will be shrunk to the nodal point $\boldsymbol{x}(I)$. The first assumption on circular arc S_ε, is that any displacement component at a nodal point is single-valued. The second assumption is that there is not a singular force acting at that nodal point. The integrals of $t^k{}_l(\boldsymbol{x},\boldsymbol{y})$ functions over the circular arc coincide with C_{kl} [4] for some special cases. After all these assumptions, Eq. (16) is reduced to a system of linear algebraic equations as below:

$$\boldsymbol{AU} = \boldsymbol{K} \tag{20}$$

where $\boldsymbol{A}$ is a $2N$ by $2N$ matrix, and whose components defined as

$$A_{IJ} = \delta_{IJ}\int_{S_\varepsilon} t_1^1(\boldsymbol{x},\boldsymbol{x}(J))ds$$

$$+\int_0^{l(J)}\{t_1^1(\boldsymbol{x},\boldsymbol{x}(I))[1-\frac{s}{l(J)}]\}ds$$

$$+\int_0^{l(J-1)}\{t_1^1(\boldsymbol{x},\boldsymbol{x}(I))[\frac{s}{l(J-1)}]\}ds$$

$$A_{I(J+N)} = \delta_{IJ}\int_{S_\varepsilon} t_2^1(\boldsymbol{x},\boldsymbol{x}(J))ds+$$

$$\int_0^{l(J)}\{t_2^1(\boldsymbol{x},\boldsymbol{x}(I))[1-\frac{s}{l(J)}]\}ds$$

$$+\int_0^{l(J-1)}\{t_2^1(\boldsymbol{x},\boldsymbol{x}(I))[\frac{s}{l(J-1)}]\}ds$$

$$A_{(I+N)J} = \delta_{IJ}\int_{S_\varepsilon} t_1^2(\boldsymbol{x},\boldsymbol{x}(J))ds+$$

$$\int_0^{l(J)}\{t_1^2(\boldsymbol{x},\boldsymbol{x}(I))[1-\frac{s}{l(J)}]\}ds$$

$$+\int_0^{l(J-1)}\{t_1^2(\boldsymbol{x},\boldsymbol{x}(I))[\frac{s}{l(J-1)}]\}ds$$

$$A_{(I+N)(J+N)} = \delta_{IJ}\int_{S_\varepsilon} t_2^2(\boldsymbol{x},\boldsymbol{x}(J))ds+$$

$$\int_0^{l(J)} \{t_2^2(\boldsymbol{x}, \boldsymbol{x}(I))[1 - \frac{s}{l(J)}]\} ds$$

$$+ \int_0^{l(J-1)} \{t_2^2(\boldsymbol{x}, \boldsymbol{x}(I))[\frac{s}{l(J-1)}]\} ds$$

$$for\ I, J = 1, N \tag{21}$$

where δ_{IJ} represents Kronecker's delta and $l(J)$ is the length of the Jth linear segment. $\boldsymbol{U}$ and $\boldsymbol{K}$ are matrices of order $2N$ by 1 defined as

$$U_I = u_1(\boldsymbol{x}(I)) \quad for\ I = 1, N$$

$$U_{(I+N)} = u_2(\boldsymbol{x}(I)) \quad for\ I = 1, N$$

$$K_I = \sum_{J=1}^{N} \int_0^{l(J)} [u_1^1(\boldsymbol{x}, \boldsymbol{x}(I))\, t_1(\boldsymbol{x})$$

$$+ u_2^1(\boldsymbol{x}, \boldsymbol{x}(I))\, t_2(\boldsymbol{x})] ds \quad for\ I = 1, N$$

$$K_{I+N} = \sum_{J=1}^{N} \int_0^{l(J)} [u_1^2(\boldsymbol{x}, \boldsymbol{x}(I))\, t_1(\boldsymbol{x})$$

$$+ u_2^2(\boldsymbol{x}, \boldsymbol{x}(I))\, t_2(\boldsymbol{x})] ds \quad for\ I = 1, N \tag{22}$$

Before limit process ($\varepsilon \to 0$) the integrals over a circular arc S_ε, see Fig. 2, about a nodal point $\boldsymbol{x}(I)$ are reduced to the calculation of the integral given below.

$$I_\lambda = \int_{\theta_1}^{\theta_2} (\mu_\lambda n_1 - n_2) \frac{1}{z_\lambda}\, ds \tag{23}$$

Substituting $n_1 = -cos\theta$, $n_2 = -sin\theta$, $z_\lambda = \varepsilon\, cos\theta + \varepsilon \mu_\lambda\, sin\theta$ and $ds = -\varepsilon d\theta$

$$I_\lambda = ln\sqrt{cos^2\theta + {\mu_\lambda}^2 sin^2\theta + 2\mu_\lambda cos\theta\, sin\theta}$$
$$+ i\, arctan(\frac{Im(\mu_\lambda\, sin\theta)}{cos\theta + Re(\mu_\lambda\, sin\theta)})\Big|_{\theta_1}^{\theta_2} \tag{24}$$

is obtained. In order to calculate the imaginary part of this integral, the following algorithm is developed:

for $\theta_2 - \pi \le \theta_1$ $\quad\quad$ $\phi_2 = \theta_2$
for $\theta_2 - \pi > \theta_1$ $\quad\quad$ $\phi_2 = -(2\pi - \theta_2)$

for $\theta_1 - \pi < \theta_2$ $\quad\quad$ $\phi_1 = \theta_1$
for $\theta_1 - \pi \ge \theta_2$ $\quad\quad$ $\phi_1 = -(2\pi - \theta_1)$

$$\beta_1 = arctan\frac{Im(\mu_\lambda) sin\phi_1}{cos\phi_1 + Re(\mu_\lambda) sin\phi_1}$$

$$\beta_2 = arctan\frac{Im(\mu_\lambda) sin\phi_2}{cos\phi_2 + Re(\mu_\lambda) sin\phi_2}$$

for $(\beta_2 - \beta_1) < 0$ $\quad\quad$ $Im(I_\lambda) = \beta_2 - \beta_1$

for $(\beta_2 - \beta_1) \ge 0$ $\quad\quad$ $Im(I_\lambda) = \beta_2 - \beta_1 - 2\pi$

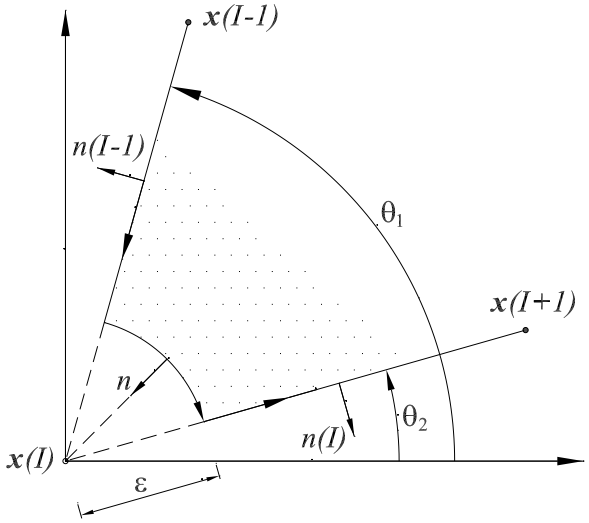

Fig. 2.
Representation of the circular arc S_ε

Other integrals over line segments (Fig. 3) in Eqs. (21) can be reduced to the combination of the following two integrals:

$$R_\lambda = \int_0^{l(J)} \frac{1}{z_\lambda} (\mu_\lambda n_1 - n_2) ds = \mid ln(z_\lambda)|_{s=0}^{l(J)}$$

$$Q_\lambda = \int_0^{l(J)} \frac{1}{z_\lambda} (n_1 \mu_\lambda - n_2) \frac{s}{l(J)} ds =$$

$$\left| lnz_\lambda \frac{s}{l(J)} - \frac{z_\lambda (lnz_\lambda - 1)}{l(J)(\mu_\lambda n_1 - n_2)} \right|_{s=0}^{l(J)} \tag{25}$$

where

$$z_\lambda = -n_2 s + x_1(J) - x_1(I)$$

$$+ \mu_\lambda (n_1 s + x_2(J) - x_2(I))$$

$$dz_\lambda = (\mu_\lambda n_1 - n_2) ds \tag{26}$$

It is seen from Eqs. (25) that another difficulty arises in the calculation of the end values of multi-valued function $ln(z_\lambda)$. To calculate their imaginary parts, an archive function program has been written to calculate all of the values of the *arctan* function on the interval $[0, 2\pi]$. This makes possible to achieve a single value for *arctan* function in this interval.

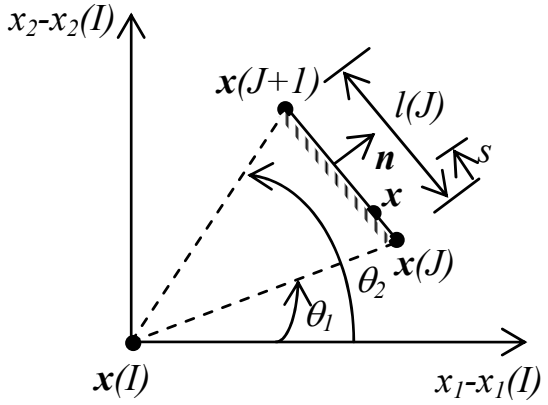

Fig. 3.
The boundary element of the number J

Then, the following algorithm is introduced:

$$Im(ln(z_\lambda)) = \phi_2 - \phi_1 \qquad (27)$$

where $\beta_1 = arctan(\frac{sin\theta_1 Im\mu_\lambda}{cos\theta_1 + sin\theta_1 Re\mu_\lambda})$,

$\beta_2 = arctan(\frac{sin\theta_2 Im\mu_\lambda}{cos\theta_2 + sin\theta_2 Re\mu_\lambda})$

for $\beta_1 > \beta_2$ $\quad \phi_2 = \beta_2$
for $\beta_1 \geq \beta_2 + \pi \Rightarrow$ $\phi_1 = -(2\pi - \beta_1)$
for $\beta_1 < \beta_2 + \pi \Rightarrow$ $\phi_1 = \beta_1$
for $\beta_1 = \beta_2 \Rightarrow$ $\quad \phi_2 = \beta_2$
$\phi_1 = \beta_1$
for $\beta_1 < \beta_2$ $\quad \phi_1 = \beta_1$
for $\beta_2 \leq \beta_1 + \pi \Rightarrow$ $\quad \phi_2 = \beta_2$
for $\beta_2 > \beta_1 + \pi \Rightarrow$ $\quad \phi_2 = -(2\pi - \beta_2)$

Since z_λ is a single-valued function using the same way the imaginary part of Q_λ can also be calculated. A third difficulty arises in the calculation of the real part of R_λ. This term involves a singularity on each of the two line segments joining at a nodal point on which a singular loading exists in any direction. But the coefficient of any displacement component at this nodal point, in the linear algebraic equation which corresponds to the loading at the same point, does not involve any singularity because the singular terms arising in adjacent elements eliminate each other. Following this algorithm all integrals over the line segments can be calculated analytically. After determination of the matrices, $\boldsymbol{A}$ and $\boldsymbol{K}$, the unknown matrix $\boldsymbol{U}$ is calculated by solving Eq. (20). For calculation of any strain component at any $\boldsymbol{y}$ point, to use the calculated nodal values of the displacement components in Eq. (17) is enough. New integrals, arising in this process, can be reduced to the same integrals mentioned above by partial integration. There are some other integrals, but they are single-valued.

If the loading point $\boldsymbol{y}$ is on the boundary, this corresponds to the case of $\theta_1 = \theta_2 \pm \pi$ which considered before, (see, Fig. 3), during calculation of $Im(R_\lambda)$. Here, there is only one restriction that it is not possible to calculate the stress components at the nodal points. If it is needed to calculate the stress components at a point, this point must not be selected as a nodal point. And if there is a singular force applied at a point on the boundary, this point cannot be selected as a nodal point either because of our second assumption on circular arc, S_ε.

4 Sample Problem

The sample problem is a square orthotropic plate, having an elliptical hole, stretched by forces parallel to x_2 axis (Fig. 4) and material constants are given in Table 1. The sample problem was selected to compare the present method with the other theoretical [1-3] and numerical study [5].

The region of the problem is multiply connected. $4N$ nodal points are selected on the boundary and the whole boundary is considered. It seems that the number of the nodal points is more than that employed in each of the other studies, but by taking advantage of the existing quarter symmetry the number of equations to be solved is reduced from $8N$ to $2N$. It must be emphasized that there is not any nodal point inside the region.

The equation of an elliptical contour in the parametric form is $x = acos\vartheta$, $y = bsin\vartheta$, where a and b are the lengths of the principal semi-axes of the ellipse, and ϑ is the parameter which assumes all values from zero to 2π for a

complete circuit of the contour. The theoretical solution of this problem for an infinite plate was also solved by Lekhnitskii [1-3]. If the semi-axes a and b of the ellipse are relatively small in comparison to l, the value of stress component $T_{\vartheta\vartheta}/p_o$ at point A must approach from above to the theoretical result given by Lekhnitskii for an infinite plate. To verify this, $T_{\vartheta\vartheta}(A)/p_o$ and $T_{\vartheta\vartheta}(B)/p_o$ values were calculated for different ratios of a/b for material I and $l = 100$ cm, $b = 0.5$ cm (Table 2). It is interesting that $T_{\vartheta\vartheta}(B)/p_o$ remains nearly constant for different a values. Lekhnitskii' s result for $T_{\vartheta\vartheta}(B)/p_o$ has also been found out to be independent from a/b ratio for an infinite plate and for material I being equal 1.4142. The variation of $T_{\vartheta\vartheta}(\theta)/p_o$ was also calculated on the boundary of the elliptical cavity by choosing $l = 100$ cm, $a = 0.7$ cm and $b = 0.5$ cm (Fig. 5). It must be emphasized that θ indicates the polar angle.

Table 1. Material Constants $(1/MPa)$

β_{11}	1/12000
β_{22}	1/6000
β_{12}	-0.071/12000
β_{66}	1/700

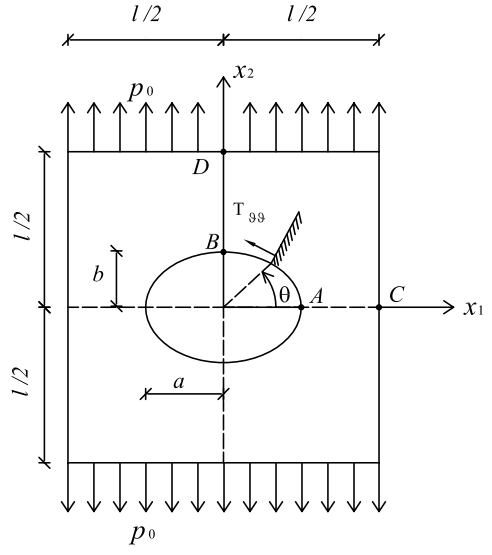

Fig. 4.
Sample problem

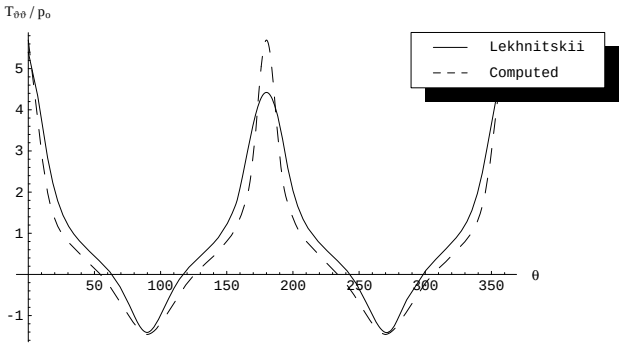

Fig. 5.
Variation of dimensionless stress component, $T_{\vartheta\vartheta}(\theta)/p_o$, versus θ, on the elliptical cavity, a=0.7 cm, b=0.5 cm and l=100 cm

Table 2.
Variations of Dimensionless Stress Components, $T_{\vartheta\vartheta}(A)/p_o$ and $T_{\vartheta\vartheta}(B)/p_o$, with the Ratio of a/b for the Elliptical Cavity, b=0.5 cm and l=100 cm

	Present Solution		Lekhnitskii
a/b	$T_{\vartheta\vartheta}(A)/p_o$	$T_{\vartheta\vartheta}(B)/p_o$	$T_{\vartheta\vartheta}(A)/p_o$
1.2	5.0413	-1.4541	4.78
1.4	5.6954	-1.4591	5.4104
1.6	6.3283	-1.4596	6.040
1.8	6.9381	-1.4579	6.6706
2	7.5239	-1.455	7.307
2.2	8.085	-1.4515	7.9307
2.4	8.622	-1.4476	8.5608
2.6	9.7087	-1.4376	9.1909
2.8	10.3601	-1.4357	9.821
3	11.0025	-1.434	10.451
3.2	11.6351	-1.4324	11.0811
3.4	12.2575	-1.431	11.7111
3.6	12.8693	-1.4296	12.3412
3.8	13.4704	-1.4284	12.9713
4	14.0605	-1.4273	13.6013

The same problem has been solved by Ref. [5] with $a/b = 4$ and $l = 20a$ and the same material. They have given the variation of the stress component T_{22}/p_o along both a vertical and an horizontal lines. In their study, the starting points of these two lines are very close to each other but not T_{22}/p_o values on them. It should be noted that the material constants have been given in

psi in their study. In order to compare the presented results with those obtained by Ref. [5], the variations of dimensionless stress component T_{22}/p_o were calculated along these specific lines by choosing $a = 5$ cm with the same a/b and a/l ratios and shown in Figs. 6 and 7 and Tables 3 and 4.

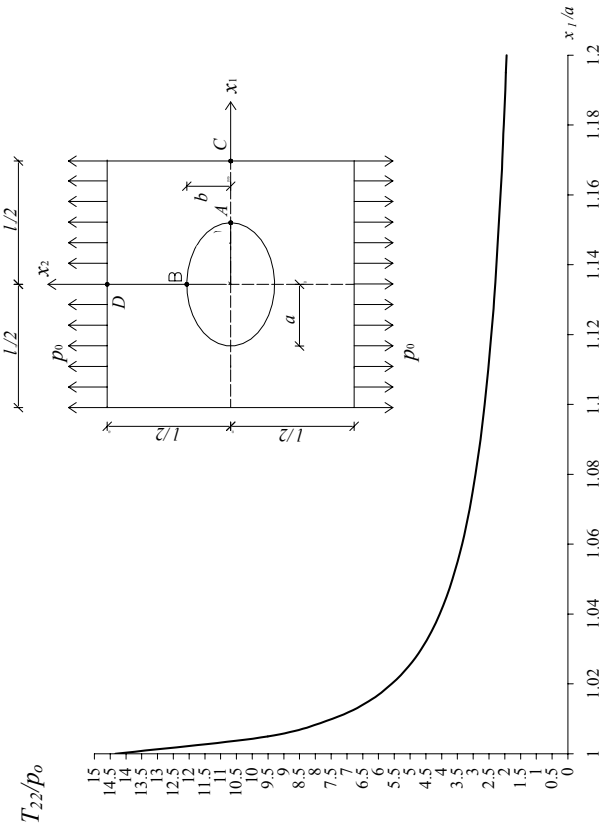

Fig. 6.

Variation of dimensionless stress component, T_{22}/p_o, along the horizontal symmetry axis for sample problem, a=5 cm and l=100 cm

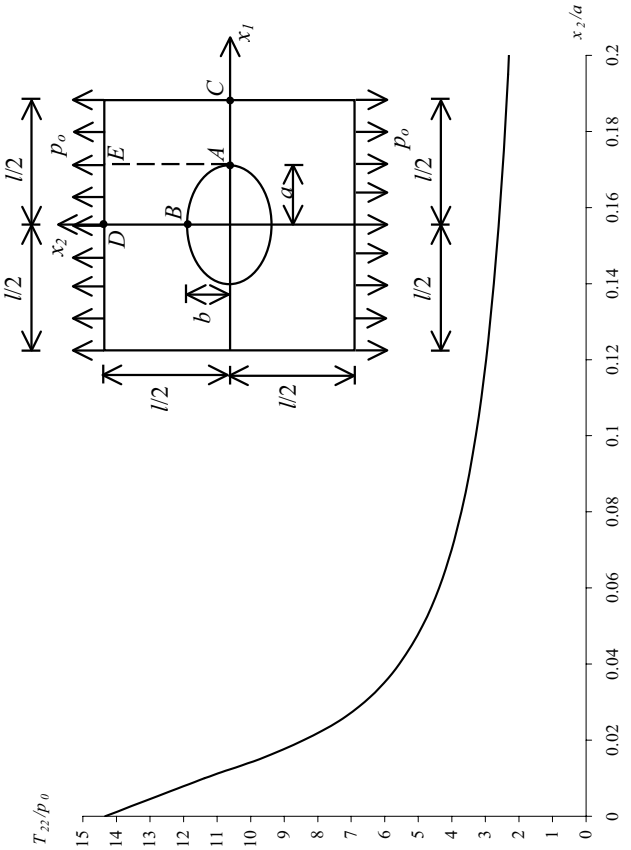

Fig. 7.

Variation of dimensionless stress component, T_{22}/p_o, along the line AE

Table 3.

Variation of Dimensionless Stress Component, T_{22}/p_o, along the Horizontal Symmetry Axis

x_1/a	T_{22}/p_o
1	14.33708
1.005	9.507749
1.01	7.456024
1.015	6.321028
1.02	5.578929
1.025	5.046719
1.03	4.641871
1.035	4.321044
1.04	4.059035
1.045	3.840065
1.05	3.653693
1.055	3.492701
1.06	3.351916
1.065	3.227528
1.07	3.116655
1.075	3.017076
1.08	2.927048
1.085	2.845178
1.09	2.770342
1.095	2.70162
1.1	2.638251
1.105	2.579599
1.11	2.525129
1.115	2.474385
1.12	2.426979
1.125	2.382575
1.13	2.340885
1.135	2.301654
1.14	2.264662
1.145	2.229714
1.15	2.196637
1.155	2.165281
1.16	2.135507
1.165	2.107196
1.17	2.080237
1.175	2.054533
1.18	2.029994
1.185	2.006542
1.19	1.984102
1.195	1.96261
1.2	1.942003

Table 4.
Variation of Dimensionless Stress Component, T_{22}/p_o, along AE Line

	T_{22}/p_o			
	Raju et. al			
x_2/a	Present	1	2	3
0	14.33708			
0.001	13.21895	8.696	8.692	8.697
0.01	11.37188	8.134	8.134	8.137
0.02	8.422955	6.934	6.935	6.934
0.03	6.603969	5.775	5.776	5.780
0.04	5.566324	4.891	4.891	4.896
0.05	4.876935	4.257	4.258	4.262
0.06	4.383839	3.797	3.798	3.803
0.07	4.011685	3.454	3.455	3.460
0.08	3.719406	3.189	3.190	3.195
0.09	3.482877	2.978	2.979	2.985
0.1	3.286951	2.806	2.807	2.813
0.11	3.121589			
0.12	2.979847			
0.13	2.856755			
0.14	2.748655			
0.15	2.652792			
0.16	2.567049			
0.17	2.489771			
0.18	2.419648			
0.19	2.355631			
0.2	2.296869			

5 Conclusions and Discussions

A few improvements are introduced to the solutions of plane problems of linear orthotropic elasticity by boundary element method. This theorem gives an integral equation for a first boundary-value problem. Unknowns of this integral equation are the boundary values of the displacement components. This integral equation can be solved using boundary elements. The aim of this study is to eliminate all of the singularities which occur during the reduction of this integral equation to a system of linear algebraic equations. To eliminate the singularities, at first, an artificial boundary for each nodal point is defined. This boundary involves boundary elements and a small arc centered at a nodal point, but, the location of this nodal point must remain outside of the artificial boundary during this process. This artificial

boundary eliminates $\boldsymbol{C}$ matrix in classical boundary element formulation. Here, the integrals, over boundary elements and the added small arc, have been determined analytically. This small arc was shrunk to the nodal point after the calculation of the required integrals over it. It is assumed that the displacement components are constant, but no stress on this small arc. The singularities arising during calculation of the integrals over adjacent elements at the nodal point are mutually eliminated. In this study, the number of nodal points has been selected to keep the element length constant for different examples. This constant length is determined by trying a different number of boundary elements for each problem. The required element length is achieved if the results remain nearly constant for a further increment in the number of boundary elements. Kernels of the integral equation mentioned above are complex. An algorithm is introduced for the calculation of the multi-valued complex integrals over the boundary elements and the small arc mentioned above. After finding the displacement components on the boundary, the unknown stress or any displacement component can be calculated on any point inside or on the boundary without any singularity problem. But, in this case, the term corresponding $\boldsymbol{C}$ matrix will be taken to be equal to unity instead of zero. There is a difficulty to calculate the unknown stress component on the boundary in classical formulation, which is named as boundary layer effect [9]. There is no boundary layer effect in this study. There are two restrictions in this method. Stresses cannot be calculated at a nodal point. And, if a singular load exists at any point on the boundary, this point must not be selected as a nodal point either because of second assumption on circular arc about a nodal point. A specific problem is selected to check the accuracy of the presented formulation and for comparison with other studies. Analytical solutions of these problems have been given by Lekhnitskii for an infinite plate. Results are compatible with those of Lekhnitskii. Moreover, the present results seem better than that of the other cited. Their results were also indicated for comparison.

References

[1] S.G. Lekhnitskii, *Anisotropic plates*, Goverment Publishing House, M-L (Russian edition), 1947

[2] S.G. Lekhnitskii, *Theory of elasticity of an anisotropic elastic body*, Holden-Day, Inc., 1963

[3] S.G. Lekhnitskii, *Anisotropic plates*, Gordon and Breach, 1968

[4] V. Mantic, and F. Paris, Explicit formulae of the integral kernels and C-matrix in the Somigliana identity for orthotropic materials, *Eng. Anal. with Bound. Elem.*, Vol. 15, No. 3, 1995, pp. 283-288.

[5] I.S. Raju, R. Sistla, and T. Krishnamurthy, An efficient boundary element method for computing accurate stresses in two-dimensional anisotropic problems, *Comput. & Struct.* , Vol. 59, No. 3, 1996, pp. 453-462.

[6] N. Kadioglu, and S. Ataoglu, An extension of boundary element method for multiply connected regions, *Boundary Elements XXI*, 1999, pp. 249-258.

[7] N. Kadioglu, and S. Ataoglu, An extension of the boundary element method in orthotropic materials for multiply connected regions, *Boundary Elements XXIII*, 2001, pp. 423-432.

[8] I.S. Sokolnikoff, *Mathematical theory of elasticity*, McGraw-Hill, 1956

[9] R.V. Avila, V. Mantič, and F. París, Application of the boundary element method to elastic orthotropic materials in 2D: numerical aspects, *Proc. Boundary Elements XIX*, 1997, pp. 55-64.